NANO LETTERS

Letter

pubs.acs.org/NanoLett

Magnetic Field-Controlled Lithium Polysulfide Semiliquid Battery with Ferrofluidic Properties

Weiyang Li,[†] Zheng Liang,[†] Zhenda Lu,[†] Xinyong Tao,[†,‡] Kai Liu,[†] Hongbin Yao,[†] and Yi Cui*[,†,§]

[†]Department of Materials Science and Engineering, Stanford University, Stanford, California 94305, United States

[‡]College of Materials Science and Engineering, Zhejiang University of Technology, Hangzhou 310014, China

[§]Stanford Institute for Materials and Energy Sciences, SLAC National Accelerator Laboratory, 2575 Sand Hill Road, Menlo Park, California 94025, United States

Supporting Information

ABSTRACT: Large-scale energy storage systems are of critical importance for electric grids, especially with the rapid increasing deployment of intermittent renewable energy sources such as wind and solar. New cost-effective systems that can deliver high energy density and efficiency for such storage often involve the flow of redox molecules and particles. Enhancing the mass and electron transport is critical for efficient battery operation in these systems. Herein, we report the design and characterization of a novel proof-of-concept magnetic field-controlled flow battery using lithium metal-polysulfide semiliquid battery as an example. A biphasic magnetic solution containing lithium polysulfide and magnetic nanoparticles is used as catholyte, and lithium metal is used as anode. The catholyte is composed of two phases of polysulfide with different concentrations, in which most of the polysulfide molecules and the superparamagnetic iron oxide nanoparticles can be extracted together to form a high-concentration polysulfide phase, in close contact with the current collector under the influence of applied magnetic field. This unique feature can help to maximize the utilization of the polysulfide and minimize the polysulfide shuttle effect, contributing to enhanced energy density and Coulombic efficiency. Additionally, owing to the effect of the superparamagnetic nanoparticles, the concentrated polysulfide phase shows the behavior of a ferrofluid that is flowable with the control of magnetic field, which can be used for a hybrid flow battery without the employment of any pumps. Our innovative design provides new insight for a broad range of flow battery chemistries and systems.

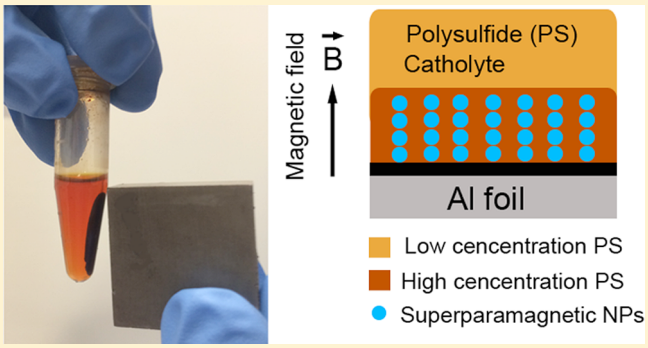

KEYWORDS: *flow battery, superparamagnetic nanoparticles, ferrofluid, lithium polysulfide battery, large-scale energy storage*

Efficient and cost-effective large-scale energy storage systems are of critical importance for electric grids, especially with the rapid increasing deployment of renewable energy sources including wind and solar that can suffer from their intermittent nature.[1−5] Among the various energy storage technologies, flow batteries are particularly attractive for such storage owing to their design flexibility and scalability, in which the fluids containing active materials can be stored in external reservoirs and pumped through a power stack to provide electricity.[6−10] This decoupling of energy and power offers great advantages of reducing the cost at large scales. Conventional aqueous-based flow battery systems,[6,7,9,10] such as vanadium redox batteries, typically operate at low voltages (<1.5 V, limited by electrolyte hydrolysis) and have limited solubility of reactant molecules (<2 M), resulting in low energy densities. They also require expensive components such as ion-selective membranes, making the realization of a desirable system cost below $100/kWh for grid storage rather challenging.[11]

Accordingly, many new cell architectures and chemistries for flow batteries have been explored to increase the energy density and decrease the system cost,[12−23] especially those can work in nonaqueous electrolytes that can yield higher operating voltage. All-organic nonaqueous redox couples have been investigated;[12,13] however, the low concentration of organic redox molecules in organic electrolytes limited their further improvement in energy density. Semisolid flow cell using colloidal suspensions composed of Li-ion compounds to replace traditional liquid catholytes and anolytes have been developed.[14−17] Nanoscale conductors were added to these solid suspensions to wire the active Li-ion compounds. On one hand, the semisolid design can deliver increased energy density with increasing loading of solid suspensions without the use of expensive membrane. However, on the other hand, this design

Received: July 16, 2015
Revised: September 11, 2015

DOI: 10.1021/acs.nanolett.5b02818
Nano Lett. XXXX, XXX, XXX−XXX

could result in slow kinetics due to the high interfacial impedance and poor contacts between particles. The high loading of solids also causes unsatisfactory flowability and, thus, produces parasitic pumping losses that reduce the system efficiency. Recently, our group developed a membrane-free semiliquid battery using lithium polysulfide solution as catholyte (with a concentration up to 7 M) and metallic lithium as anode, which can provide high energy density at low cost (~72 Wh/L at 5 M; $45/kWh for raw materials).[18] However, in order to maximize the utilization of the active polysulfide at such high concentration, large amount of porous carbon felt or carbon fiber paper had to be employed as current collector, in which their pores can be blocked by the discharged product, building up high driving pressure for the pump. Instead of using porous carbon as current collector, Fan et al. further extended this system to lithium polysulfide hybrid flow battery by incorporating conductive carbon nanoparticles with the polysulfide fluids to form an embedded current collector.[19] Besides the sufficient carbon nanoparticles added to ensure the utilization of polysulfide, gold-sputtered current collector was used to further improve the contact with polysulfide, which increased the system cost. Similar issue occurs here for the pump as high solution molarity leads to high solution viscosities, causing large flow resistance and pump losses.

Along this line, the development of new energy system that can deliver high energy density and efficiency for grid storage is highly desirable. This system should include the following two attributes: (*i*) maximizing the utilization of the electrochemically active molecules; (*ii*) minimizing the pump losses. Herein we report the design and characterization of an innovative proof-of-concept magnetic field-enhanced semiliquid lithium polysulfide (Li-PS) battery, as illustrated in Figure 1. We note

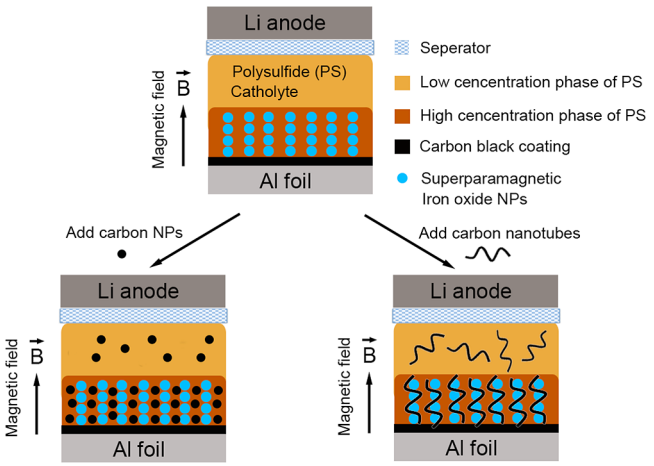

Figure 1. Schematic illustrating the proof-of-concept magnetic field-controlled semiliquid battery. A biphasic magnetic solution containing lithium polysulfide and magnetic nanoparticles (NPs) is used as catholyte, and lithium metal is used as anode. The catholyte is composed of two phases, where the polysulfide and the superparamagnetic iron oxide NPs can be extracted together to a phase in close contact with the current collector under the influence of applied magnetic field. Owing to the effect of the superparamagnetic NPs, the concentrated polysulfide phase shows the behavior of a ferrofluid that is flowable with the control of the magnetic field. Aluminum foil coated with conductive carbon black is used as the current collector. Nanoscale conductors, such as carbon NPs or carbon nanotubes can be incorporated into the catholyte to form conductive networks so as to improve the conductivity of the catholyte.

that the concept of using magnetic field to enable the control of mass transport is not limited to lithium polysulfide and can also be exploited for other flow battery systems. A biphasic magnetic solution containing lithium polysulfide (Li_2S_8) and magnetic nanoparticles (NPs) is used as catholyte, and lithium metal is used as anode. Aluminum foil coated with conductive carbon black is used as the current collector. The catholyte is composed of two phases, where the Li_2S_8 and the superparamagnetic iron oxide NPs can be extracted together to form a phase in close contact with the current collector under the influence of applied magnetic field. This generates a concentration difference, in which a phase of Li_2S_8 at high concentration can be fixed at the side of cathode current collector in the cell, leaving a phase of Li_2S_8 at low concentration to the anode side. Previous research of typical lithium−sulfur batteries showed that soluble lithium polysulfides (Li_2S_x, $4 \leq x \leq 8$) in the electrolyte could diffuse to the anode side to react with lithium metal, and shuttle between the cathode and anode, resulting in low Coulombic efficiency and rapid capacity loss.[24−26] Our unique biphasic feature can help to minimize the polysulfide shuttle effect, maximize the polysulfide utilization, and improve the contact between polysulfide and the current collector. Moreover, owing to the effect of the superparamagnetic NPs, the high-concentration polysulfide phase shows the behavior of a ferrofluid that is flowable with the control of the magnetic field. Therefore, the biphasic magnetic polysulfide catholyte can be used for a hybrid flow battery, in which no pump is required in this system and, thus, no pump loss will be involved. Nanoscale conductors, such as carbon NPs or carbon nanotubes, can be incorporated into the catholyte to form conductive networks so as to improve the conductivity and enhance the utilization of active polysulfide.

In a typical synthesis, γ-Fe_2O_3 NPs were first synthesized by a thermolysis process as previously reported.[27] As shown in the transmission electron microscopy (TEM) image in Figure 2a, these NPs are highly uniform, are narrow in size distribution, and have an average diameter of ~11 nm. The surfaces of these particles are stabilized with oleic acid and can be well dispersed in nonpolar solvent, such as toluene or cyclohexane. The as-prepared γ-Fe_2O_3 NPs exhibit the property of superparamagnetism, which means that when an external magnetic field is applied, the magnetic moments of these particles can align along the applied field, and this magnetization does not retain once the field is removed. Because of this, the colloidal γ-Fe_2O_3 solution shows a typical ferrofluidic behavior when subjected to an external magnetic field (Figure 2b). The location of the fluid can be precisely controlled via a magnetic field, and the fluid can be forced to flow by varying the strength of the field.

To prepare the biphasic magnetic polysulfide solution, a toluene suspension of the superparamagnetic γ-Fe_2O_3 NPs was mixed with the lithium polysulfide (Li_2S_8) solution (volume ratio = 1:1). The Li_2S_8 solution can be prepared by stirring stoichiometric amounts of lithium sulfide and sulfur in cosolvent of 1,2-dimethoxyethane (DME) and 1,3-dioxolane (DOL) (volume ratio = 1:1), as reported in our previous research.[18] A magnet was subsequently applied to the mixed solution. As a result, a solution with two phases was formed. As shown in Figure 2c, most of the polysulfide molecules together with γ-Fe_2O_3 NPs can be extracted to the same phase that is attracted to the magnetic field, forming a concentrated polysulfide phase. Similar to the colloidal γ-Fe_2O_3 solution (Figure 2b), the concentrated polysulfide phase also exhibit the

DOI: 10.1021/acs.nanolett.5b02818
Nano Lett. XXXX, XXX, XXX−XXX

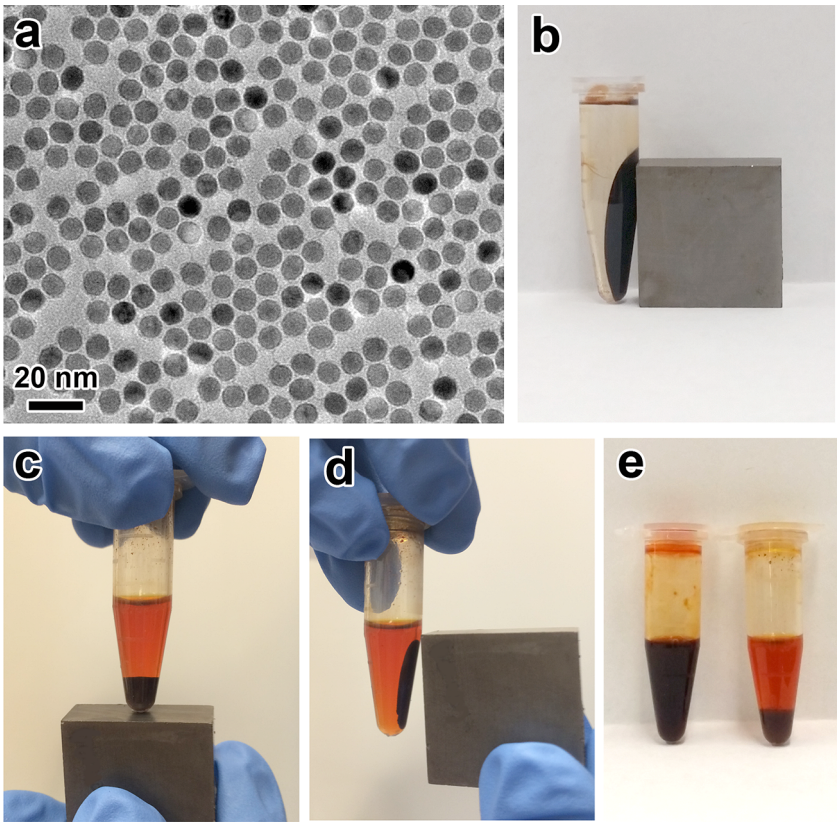

Figure 2. (a) TEM image of the superparamagnetic γ-Fe_2O_3 nanoparticles (NPs). (b) Photograph showing the ferrofluidic behavior of γ-Fe_2O_3 NPs in toluene in the presence of an external magnet (right). (c) Photograph of the biphasic magnetic polysulfide solution, where the polysulfide together with γ-Fe_2O_3 NPs can be extracted to the same phase that is attracted to the magnetic field (magnet at the bottom). (d) Photograph showing the ferrofluidic behavior of the concentrated phase containing polysulfide and the γ-Fe_2O_3 NPs in the presence of a magnet (right). (e) Photograph showing the color difference of pure polysulfide solution (left) and biphasic magnetic polysulfide solution (right) (with the same amount of polysulfide in the same volume).

characteristic of ferrofluid, and can move with the applied magnetic field (Figure 2d; also see Supporting Information Video 1), which could be attributed to the interaction between the superparamagnetic iron oxide NPs and the polysulfide. This very unique phenomenon could potential be used for a novel flow battery system controlled by magnetic field, eliminating the use of any pumps. Our previous study showed that there exists strong binding between lithium polysulfide and metal oxide materials due to the metal−sulfur interaction.[28−30] Here, similar interaction could occur between γ-Fe_2O_3 and polysulfide. In addition, because the surfaces of γ-Fe_2O_3 NPs are stabilized with oleic acid, the interaction between Li atom in Li_2S_8 and O atom in oleic acid could also contribute to the adsorption of polysulfide on the γ-Fe_2O_3 particle surface. This Li−O bonding had been demonstrated in our previous studies.[31−33] Moreover, the strong absorption of polysulfide on the surfaces of superparamagnetic γ-Fe_2O_3 NPs can also enable strong binding with the charged product of sulfur during the very last stage of the charging process (polysulfides are transformed into sulfur), which is similar to our previous demonstration of controlled sulfur deposition on tin-doped indium oxide surface.[29] Figure 2e displays the color difference of pure polysulfide solution (left) and biphasic magnetic polysulfide solution (right) (with the same amount of polysulfide), clearly showing that polysulfide is mostly concentrated in the lower phase of the biphasic magnetic polysulfide solution that is attracted to the magnet.

To test the electrochemical properties of the biphasic magnetic polysulfide catholyte, galvanostatic charge−discharge measurements were performed. We used 2032-type coin cells (MTI) to evaluate the performance of this proof-of-concept magnetic field-enhanced semiliquid cell. The cells were assembled with lithium foil as the anode and the biphasic magnetic polysulfide solution as the catholyte. Aluminum foil, which was coated with a layer of carbon black (Ketjenblack EC-600JD, AzkoNobel, referred to as KB), was used as the current collector for the catholyte. A magnet was placed close to the cathode side of the cell during the electrochemical measurements. Control cells were fabricated using lithium polysulfide solution (dissolved in DOL/DME) as catholyte without γ-Fe_2O_3 NPs. In each coin cell, same volume of catholyte (60 μL) containing the same amount of lithium polysulfide was added (Li_2S_8, 2.5 M, calculated based on the mass of sulfur). Lithium bis(trifluoromethanesulfonyl)imide (LiTFSI) with a concentration of 0.5 M and 1 wt % of lithium nitrate ($LiNO_3$) were also dissolved in DOL/DME with the Li_2S_8. The amount of γ-Fe_2O_3 NPs in the catholyte is 0.015 mg/uL. The amount of KB NPs or carbon nanotubes added in the catholyte is 10^{-3} mg/uL. The cells are cycled in a voltage range of 2.13−2.6 V, as in our previous reported lithium polysulfide semiliquid battery.[18] This means that the catholyte is cycled between sulfur and electrolyte-soluble Li_2S_4 phase, not discharged to the insoluble lithium sulfide phases (Li_2S_2/Li_2S) so as to avoid the issue of poor kinetics of Li_2S/Li_2S in conventional Li−S batteries. In all measurements, the current density (C rate) is defined based on

DOI: 10.1021/acs.nanolett.5b02818
Nano Lett. XXXX, XXX, XXX−XXX

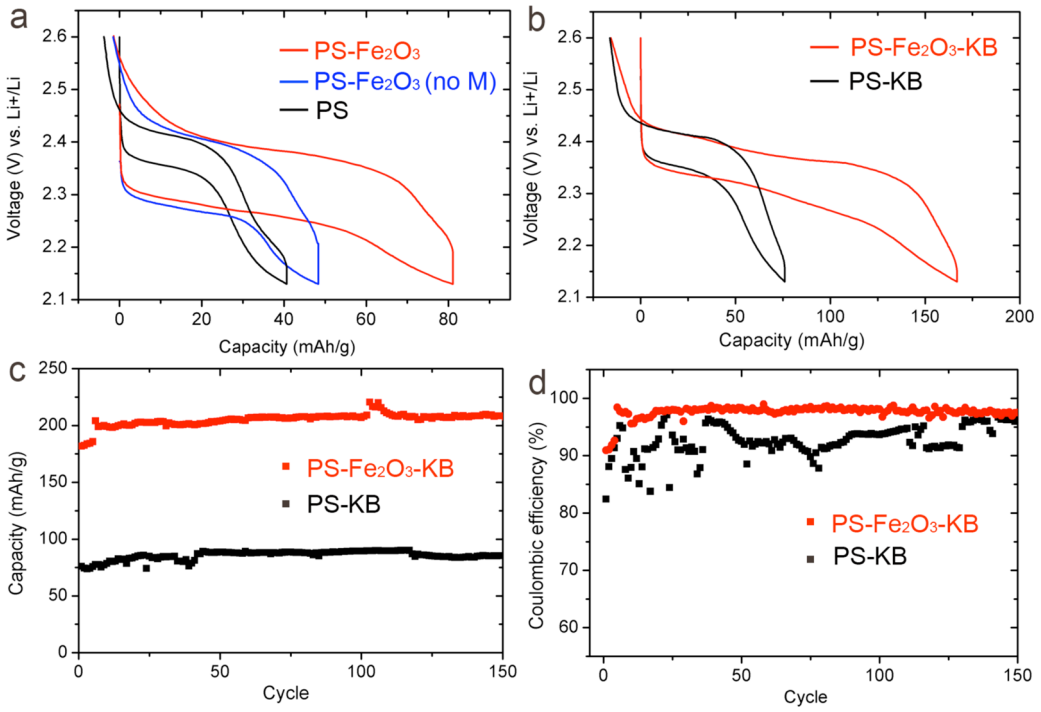

Figure 3. (a) Discharge−charge voltage profiles during the 2nd cycle of cells made from the biphasic magnetic polysulfide catholyte containing the γ-Fe_2O_3 NPs with (PS-Fe_2O_3, red line) and without the applied magnetic field (PS-Fe_2O_3, no M, where M refers to magnetic field; blue line), measured at a current density of 0.2C. The control cell made from polysulfide solution (PS, black line) is also shown in (a). (b) Discharge−charge voltage profiles during the 2nd cycle of cells made from the biphasic magnetic polysulfide catholyte containing γ-Fe_2O_3 and KB NPs with applied magnetic field (referred to as PS-Fe_2O_3−KB, red line) and the control cell made from the polysulfide catholyte containing KB alone (referred to as PS−KB, black line). (c) Discharge capacity and (d) Coulombic efficiency vs cycle number of the PS-Fe_2O_3−KB (red square) and PS−KB (black square) catholytes, respectively.

the theoretical capacity (418 mAh/g) between S and Li_2S_4 (based on the mass of sulfur in the catholyte; 1C = 418 mA/g).

Figure 3a shows the typical discharge−charge voltage profiles during the second cycle of cells made from the biphasic magnetic polysulfide catholyte containing the γ-Fe_2O_3 NPs (referred to as PS-Fe_2O_3) with and without the applied magnetic field (indicated as no M in the figure), measured at a current density of 0.2C. For comparison, the discharge−charge curve of control cell made from polysulfide solution only (referred to as PS), measured at the same current density, is also shown in Figure 3a. It can be observed that with the applied field, the PS-Fe_2O_3 catholyte delivers a capacity of 82 mAh/g, which is more than twice higher than that of the PS solution (only ∼40 mAh/g). However, without the magnetic field, the PS-Fe_2O_3 catholyte exhibits similar discharge capacity as the PS solution. This clearly indicates the effect of the magnetic NPs, which are attracted to the magnetic field and help to concentrate the polysulfide close to the current collector. The Coulombic efficiency (CE) of the cells made from PS-Fe_2O_3 catholyte is 98.3% and 96.8% with and without magnetic field at this cycle, respectively, whereas the CE of the cell made from PS is only 91.5%. This reveals that the magnetic NPs can help to greatly reduce the polysulfide shuttle effect, especially under the control of the magnetic field. The magnetic NPs can anchor the polysulfides at the cathode side, preventing them from shuttling to the anode. It is noted that the voltage hysteresis of the PS-Fe_2O_3 catholyte is around 50 mV higher than that of the PS catholyte, which could be due to the decrease in the conductivity of the catholyte due to the nonconductive nature of the Fe_2O_3 NPs.

To improve the conductivity of the catholyte and the polysulfide utilization, conductive carbon black particles were added to the catholyte as conducting networks. Figure 3b shows a comparison of the discharge−charge voltage profiles during the second cycle of cells made from the biphasic magnetic polysulfide catholyte containing γ-Fe_2O_3 and KB NPs with applied magnetic field (referred to as PS-Fe_2O_3−KB) and the control cell made from the polysulfide catholyte containing KB alone (referred to as PS−KB), measured at a current density of 0.2C. It can be seen that the cells at both conditions can deliver much higher capacities compared with that of the cells without KB in Figure 3a. With the applied magnetic field, PS-Fe_2O_3−KB catholyte gives a capacity of ∼168 mAh/g, whereas the PS−KB one only exhibits a capacity of 75 mAh/g. It is also noticed that the voltage hysteresis for PS-Fe_2O_3−KB is about the same as that of PS−KB (∼70 mV). This indicates that the nonconductive nature of iron oxide has been compensated by the conductive KB NPs. As shown in Figure 3c, both cells showed stable cycling stability. The cells made from the PS-Fe_2O_3−KB and PS−KB can give a reversible capacity of 210 mAh/g and 82 mAh/g, respectively, after 150 cycles.

Figure 3d shows a comparison of the CE over cycling. Obviously, the CE of the cell made from PS-Fe_2O_3−KB shows much more improved and stable CE over cycling compared with the one from PS−KB. The average CE of the cell made from PS-Fe_2O_3−KB is 97.6% over 150 cycles, whereas the CE of the cell made from PS−KB goes up and down over cycling and the average CE over 150 cycles is only 92.6%. It is also noticed that by adding KB NPs into the polysulfide, the CE becomes lower and less stable over cycling compared with the

DOI: 10.1021/acs.nanolett.5b02818
Nano Lett. XXXX, XXX, XXX−XXX

one without the addition of KB (a comparison of the discharge−charge curves shown in Figure 3a and b; also see a comparison of CE vs cycling in Figure S1 in the Supporting Information), especially for the case when using PS−KB as catholyte. The reason could be that KB NPs in the catholyte can cross over through the separator and attach to the surface of the lithium metal anode. This can be detrimental for the formation of a stable solid electrolyte interphase (SEI) layer on the lithium anode, aggravating the growth of lithium dendrites and thus decreasing the CE. In contrast, when KB was added into the biphasic magnetic catholyte, KB NPs were first dispersed in the DOL/DME solution with polysulfide, and then mixed with the toluene suspension of γ-Fe_2O_3 NPs. In this case, in the resulting PS-Fe_2O_3−KB catholyte, the KB NPs were mostly present in the concentrated polysulfide phase instead of uniformly distributed in the whole solution (as shown in the schematic in Figure 1, lower left), which has less interference in the formation of the protective SEI layer on lithium anode and contributes to higher CE over cycling.

Instead of employing KB NPs, we further tested the effect of adding carbon nanotubes (CNTs) into the polysulfide catholyte to form the percolating conductor networks. Surprisingly, both the capacity and the CE of the cells are drastically enhanced. Figure 4a shows the discharge−charge voltage curves during the second cycle of cells made from the biphasic magnetic polysulfide catholyte containing the γ-Fe_2O_3 NPs and CNTs (denoted as PS-Fe_2O_3−CNT hereafter) with applied magnetic field, and the control cell made from the catholyte containing only a mixture of polysulfide and CNTs (denoted as PS−CNT), measured at a current density of 0.2C. The PS-Fe_2O_3−CNT can deliver a high capacity of ~350 mAh/g (close the theoretical capacity of 418 mAh/g), corresponding to a volumetric energy density of 66 Wh/L (calculated based on the volume of the catholyte), whereas the PS−CNT gives a capacity of ~126 mAh/g. This indicates that CNTs can form a better conductive network than KB NPs, owing to the interconnected nature of CNTs. It is worth mentioning that when replacing KB with CNT, the discharge capacity of PS-Fe_2O_3−CNT increased by 110% compared with that of PS-Fe_2O_3−KB shown in Figure 3b, while the discharge capacity of PS−CNT only increased by 68% compared with that of PS−KB. Moreover, as shown in Figure 4a, the cell made from PS-Fe_2O_3−CNT exhibits very small polarization. The voltage hysteresis is only ~30 mV (even smaller than that of the PS−CNT, ~ 45 mV), revealing the much more enhanced kinetics. This can be attributed to the better contact between the Fe_2O_3 NPs and CNTs. Instead of weak interparticle contact between Fe_2O_3 and KB NPs, the Fe_2O_3 NPs can be tangled together with the interconnected CNTs. Therefore, when an external magnetic field was applied, the magnetic Fe_2O_3 NPs were subject to draw most of the CNTs into the concentrated polysulfide phase, increasing the utilization of both CNTs and polysulfide and, thus, contributing to high capacity and low polarization. The capacity and CE of the cells versus cycling is displayed in Figure 4b. After 150 cycles, a reversible capacity of ~326 mAh/g can still be obtained with little capacity decay, which corresponds to a remarkable capacity retention of 93%, whereas the PS−CNT shows a capacity of ~100 mAh/g after 150 cycles (a capacity retention of 83%). The cell made from PS-Fe_2O_3−CNT also shows improved CE compared with the cell made from PS−CNT. The average CE efficiency of the cell made from PS-Fe_2O_3−CNT can be maintained over 98.1% during the 150 cycles, while the average CE of the cell made from PS−CNT over 150 cycles is 97.0%. It is also noticed that the CEs of the cells using CNTs as conductive additives are much better than the ones that used KB NPs (Figure 3d), especially the CEs for the first several cycles of the cells. This could be due to the fact that the CNTs could not cross over through the separator as small KB NPs and has less influence on the formation of a stable SEI layer on lithium metal anode.

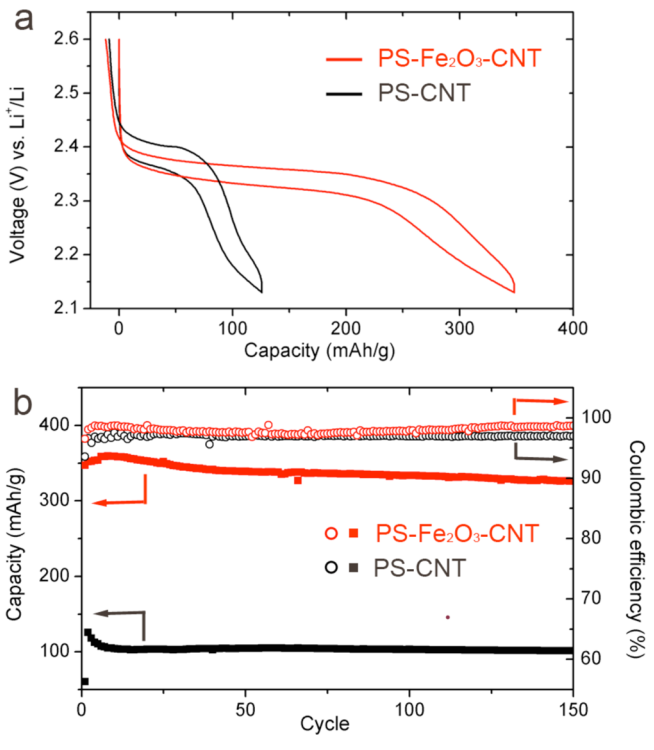

Figure 4. (a) Discharge−charge voltage curves during the 2nd cycle of cells made from the biphasic magnetic polysulfide catholyte containing the γ-Fe_2O_3 NPs and CNTs (denoted as PS-Fe_2O_3−CNT, red line) with applied magnetic field, and the control cell made from the catholyte containing only a mixture of polysulfide and CNTs (denoted as PS−CNT, black line), measured at a current density of 0.2C. (b) Discharge capacity (solid square) and Coulombic efficiency (hollow circle) vs cycle number of the PS-Fe_2O_3−CNT (red) and PS−CNT (black) catholytes, respectively.

In conclusion, we have developed an innovative magnetic field-enhanced semiliquid Li-PS battery, in which a biphasic magnetic solution containing Li_2S_8 and magnetic nanoparticles is used as catholyte, and lithium metal is used as anode. The catholyte is composed of two phases, where the Li_2S_8 and the superparamagnetic iron oxide nanoparticles can be extracted together to a phase in close contact with the current collector under the influence of applied magnetic field. This unique feature can help to minimize the polysulfide shuttle effect, maximize the utilization of the active polysulfide, and improve the contact between polysulfide and the current collector. Moreover, owing to the influence of the superparamagnetic NPs, the concentrated polysulfide phase shows the behavior of a ferrofluid that is flowable under the control of an external magnetic field, which can be used for a hybrid flow battery without the employment of any pumps and, thus, can eliminate the pump losses. Nanoscale conductors, such as carbon NPs or CNTs can be further incorporated into the catholyte to form conductive networks so as to improve the conductivity and the utilization of the catholyte. We found out that CNTs are better

DOI: 10.1021/acs.nanolett.5b02818
Nano Lett. XXXX, XXX, XXX−XXX

conductors to enable the formation of conductive networks than carbon NPs, and can contribute to higher capacity and better CE. As a result, the biphasic magnetic polysulfide catholyte can deliver a high capacity of ~350 mAh/g (close the theoretical capacity of 418 mAh/g), corresponding to a volumetric energy density of ~66 Wh/L (calculated based on the volume of the catholyte). Our novel magnetic filed-enhanced battery design provides new insights and possibilities into exploring the most promising energy systems for the grid and has great potential to be applied to other energy storage systems.

■ ASSOCIATED CONTENT

Supporting Information

The Supporting Information is available free of charge on the ACS Publications website at DOI: 10.1021/acs.nanolett.5b02818.

Coulombic efficiency of the cell made from lithium polysulfide alone. (PDF)

Video showing the ferrofluidic behavior of the concentrated phase containing lithium polysulfide and the γ-Fe_2O_3 nanoparticles in the presence of a magnet. (AVI)

■ AUTHOR INFORMATION

Corresponding Author

*E-mail: yicui@stanford.edu.

Notes

The authors declare no competing financial interest.

■ ACKNOWLEDGMENTS

This work was supported as part of the Joint Center for Energy Storage Research (JCESR), an Energy Innovation Hub funded by the U.S. Department of Energy, Office of Science, Basic Energy Sciences. We would like to thank Prof. Yadong Yin's group at UC Riverside for the help on preparing the magnetic nanoparticles.

■ REFERENCES

(1) Dunn, B.; Kamath, H.; Tarascon, J.-M. *Science* **2011**, *334*, 928−935.

(2) Yang, Z.; Zhang, J.; Kintner-Meyer, M. C. W.; Lu, X.; Choi, D.; Lemmon, J. P.; Liu, J. *Chem. Rev.* **2011**, *111*, 3577−3613.

(3) Carbajales-Dale, M.; Barnhart, C. J.; Benson, S. M. *Energy Environ. Sci.* **2014**, *7*, 1538−1544.

(4) Chu, S.; Majumdar, A. *Nature* **2012**, *488*, 294−303.

(5) Liu, J.; Zhang, J.-G.; Yang, Z.; Lemmon, J. P.; Imhoff, C.; Graff, G. L.; Li, L.; Hu, J.; Wang, C.; Xiao, J.; Xia, G.; Viswanathan, V. V.; Baskaran, S.; Sprenkle, V.; Li, X.; Shao, Y.; Schwenzer, B. *Adv. Funct. Mater.* **2013**, *23*, 929−946.

(6) Weber, A. Z.; Mench, M. M.; Meyers, J. P.; Ross, P. N.; Gostick, J. T.; Liu, Q. *J. Appl. Electrochem.* **2011**, *41*, 1137−1164.

(7) Ponce de León, C.; Frías-Ferrer, A.; González-García, J.; Szánto, D. A.; Walsh, F. C. *J. Power Sources* **2006**, *160*, 716−732.

(8) Skyllas-Kazacos, M.; Chakrabarti, M. H.; Hajimolana, S. A.; Mjalli, F. S.; Saleem, M. *J. Electrochem. Soc.* **2011**, *158*, R55−R79.

(9) Wang, W.; Luo, Q.; Li, B.; Wei, X.; Li, L.; Yang, Z. *Adv. Funct. Mater.* **2013**, *23*, 970−986.

(10) Huang, Q.; Wang, Q. *ChemPlusChem* **2015**, *80*, 312−322.

(11) ARPA-E FOA# DE-FOA-0000290. https://arpa-e-foa.energy.gov/Default.aspx?Archive=1#FoaId85e239bb-8908-4d2c-ab10-dd02d85e7d78 (accessed September, 2015).

(12) Darling, R. M.; Gallagher, K. G.; Kowalski, J. A.; Ha, S.; Brushett, F. R. *Energy Environ. Sci.* **2014**, *7*, 3459.

(13) Brushett, F. R.; Vaughey, J. T.; Jansen, A. N. *Adv. Energy Mater.* **2012**, *2*, 1390−1396.

(14) Duduta, M.; Ho, B.; Wood, V. C.; Limthongkul, P.; Brunini, V. E.; Carter, W. C.; Chiang, Y.-M. *Adv. Energy Mater.* **2011**, *1*, 511−516.

(15) Hamelet, S.; Tzedakis, T.; Leriche, J.-B.; Sailler, S.; Larcher, D.; Taberna, P.-L.; Simon, P.; Tarascon, J.-M. *J. Electrochem. Soc.* **2012**, *159*, A1360−A1367.

(16) Li, Z.; Smith, K. C.; Dong, Y.; Baram, N.; Fan, F. Y.; Xie, J.; Limthongkul, P.; Carter, W. C.; Chiang, Y.-M. *Phys. Chem. Chem. Phys.* **2013**, *15*, 15833.

(17) Wei, T.-S.; Fan, F. Y.; Helal, A.; Smith, K. C.; McKinley, G. H.; Chiang, Y.-M.; Lewis, J. A. *Adv. Energy Mater.* **2015**, *5*, n/a.

(18) Yang, Y.; Zheng, G.; Cui, Y. *Energy Environ. Sci.* **2013**, *6*, 1552−1558.

(19) Fan, F. Y.; Woodford, W.; Li, Z.; Baram, N.; Smith, K. C.; Helal, A.; McKinley, G. H.; Carter, W. C.; Chiang, Y.-M. *Nano Lett.* **2014**, *14*, 2210−2218.

(20) Demir-Cakan, R.; Morcrette, M.; Guéguen, A.; Dedryvère, R.; Tarascon, J.-M. *Energy Environ. Sci.* **2012**, *6*, 176−182.

(21) Lu, Y.; Goodenough, J. B.; Kim, Y. *J. Am. Chem. Soc.* **2011**, *133*, 5756−5759.

(22) Lu, Y.; Goodenough, J. B. *J. Mater. Chem.* **2011**, *21*, 10113−10117.

(23) Chen, H.; Zou, Q.; Liang, Z.; Liu, H.; Li, Q.; Lu, Y.-C. *Nat. Commun.* **2015**, *6*, 5877.

(24) Yang, Y.; Zheng, G.; Cui, Y. *Chem. Soc. Rev.* **2013**, *42*, 3018−3032.

(25) Manthiram, A.; Fu, Y.-Z.; Su, Y.-S. *Acc. Chem. Res.* **2013**, *46*, 1125−1134.

(26) Evers, S.; Nazar, L. F. *Acc. Chem. Res.* **2013**, *46*, 1135−1143.

(27) Hyeon, T.; Lee, S. S.; Park, J.; Chung, Y.; Na, H. B. *J. Am. Chem. Soc.* **2001**, *123*, 12798−12801.

(28) Tao, X.; Wang, J.; Ying, Z.; Cai, Q.; Zheng, G.; Gan, Y.; Huang, H.; Xia, Y.; Lian, C.; Zhang, W.; Cui, Y. *Nano Lett.* **2014**, *14*, 5288−5294.

(29) Yao, H.; Zheng, G.; Hsu, P.-C.; Kong, D.; Cha, J. J.; Li, W.; Seh, Z. W.; McDowell, M. T.; Yan, K.; Liang, Z.; Narasimhan, V. K.; Cui, Y. *Nat. Commun.* **2014**, *5*, 3943.

(30) Liang, Z.; Zheng, G.; Li, W.; Seh, Z. W.; Yao, H.; Yan, K.; Kong, D.; Cui, Y. *ACS Nano* **2014**, *8*, 5249−5256.

(31) Li, W.; Zhang, Q.; Zheng, G.; Seh, Z. W.; Yao, H.; Cui, Y. *Nano Lett.* **2013**, *13*, 5534−5540.

(32) Zheng, G.; Zhang, Q.; Cha, J. J.; Yang, Y.; Li, W.; Seh, Z. W.; Cui, Y. *Nano Lett.* **2013**, *13*, 1265−1270.

(33) Seh, Z. W.; Zhang, Q.; Li, W.; Zheng, G.; Yao, H.; Cui, Y. *Chem. Sci.* **2013**, *4*, 3673−3677.

DOI: 10.1021/acs.nanolett.5b02818
Nano Lett. XXXX, XXX, XXX−XXX